nzsee
NEW ZEALAND SOCIETY FOR EARTHQUAKE ENGINEERING

Enhancing seismic performance of existing buildings using viscous dampers for forward-directivity earthquakes: some important observations

A. M. Puthanpurayil, R D. Sharpe & R D. Jury
Beca Ltd., Wellington.

A. J. Carr, A. Murahidy
MC Consulting Engineers, Christchurch.

ABSTRACT

Enhancing the performance of an existing building with viscous dampers for a Wellington site requires thorough consideration of near-fault effects, the Wellington Fault being so close. Earthquake records with forward-directivity characteristics may have one or more significant velocity and displacement pulses. These pulses may give rise to complex inelastic dynamic mechanisms in the parent structure. To retrofit such a building using viscous dampers to improve the performance in such seismic events demands a refined design approach. The design process described in this paper follows a performance-based seismic design approach which explicitly addresses the target performance to be achieved through inelastic dynamic design of the viscously-damped structural system. While the global effect of viscous dampers in a structure is equivalent to increasing the inherent damping of the structure, the process involved is complex due to the non-classical nature of the added damping. This paper discusses applying this design methodology to an 11-storey building in Wellington. In particular, the paper discusses some observations on the performance of the structure in a near-fault event.

1 INTRODUCTION

The conventional ductile-design strategy relies on the structure absorbing seismic energy in a major earthquake by it enduring large inelastic deformations. The inelastic deformation results in heavy economic losses in the form of material damage to structural and non-structural elements. Past earthquakes have

exemplified this aspect. The impact of the M_w 7.8, 14th November 2016, Kaikoura earthquake in New Zealand is a very recent example of the economic losses mainly incurred because of the adoption of this philosophy. Although this earthquake resulted in only two deaths, the earthquake-related damage to buildings and infrastructure was roughly estimated as being greater than *NZ $*15 billion. Similarly, the damage and business disruption from the 2010 and 2011 Canterbury earthquakes amounted to greater than *NZ $*40 billion which corresponds to approximately 20 % of New Zealand's Gross Domestic Product (Pampanin 2015). This figure does not include the social-fabric disruption which would result in extensive migration of people and relocation of economic activities. Similar observations could be made from past events in other parts of the world. For example, the 1989 *M* 6.9 Loma Prieta earthquake caused more than *US $*8 billion in direct damage (several buildings and bridges suffered total and partial collapse) although no major loss of life occurred (Wada et al., 2004). Similar observations were made after the 1995 Kobe earthquake (*US $*102.5 billion in damage, 2.5 % of Japan's GDP at the time) and the 1999 Chi-Chi earthquake which caused about *US $*10 billion worth of damage (Wada et al., 2004).

One of the ways of reducing the earthquake-induced damage and ensuring life safety is to apply technologies such as viscous dampers to the structure. Viscous dampers are effective in reducing seismic responses. This is mainly attributed to the fact that the damper force is linearly or nonlinearly proportional to velocity and is out of phase with the displacements and hence peak structural forces. As a result, the columns or foundations are not subjected to additional demand and may not need to be strengthened (Constantinou *et al.,*1993).

Although the application of viscous dampers in retrofitting structures can be attractive, the design process of such a system is very complex. This paper outlines a performance-based design process for such a system. This design process is applied to the retrofitting of a building in Wellington. This paper discusses some of the existing approaches for performance-based design and draws conclusions specific to the Wellington region because of its high level of seismicity with the likelihood of forward-directivity effects. The proposed approach is likely to also be applicable for other regions with a similar, high level of seismicity and/or the likelihood of near-field effects.

2 WHAT IS A VISCOUS DAMPER?

A viscous damper is a fluid-mechanical device which induces forces proportional to the velocity which are out of phase with the structural displacements and accelerations. A typical section of a viscous damper is shown in Figure 1. The damper consists of a stainless-steel piston inside a steel cylinder which is divided into two chambers by the piston head. The cylinder is filled with a compressible hydraulic fluid and a pressure accumulator for smooth fluid circulation.

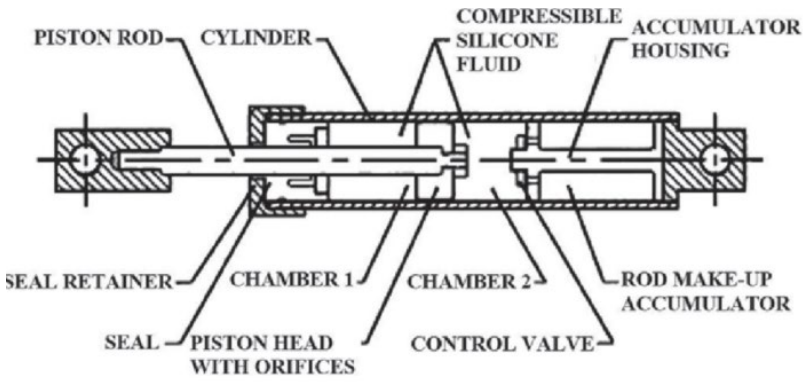

Figure 1: A typical cross section of a viscous damper (Taylor Devices inc.)

3 MODELLING OF VISCOUSLY-DAMPED STRUCTURES

The equation of motion (EOM) incorporating the viscous dampers is:

$$\boldsymbol{M\ddot{u}(t) + C_{structure}\dot{u}(t) + f_{damper}(t) + f_{NL}(t) = -MI\ddot{u}_g(t)} \quad (1)$$

where:

$\boldsymbol{M}$ represents the mass of the system,

$\boldsymbol{C_{structure}}$ represents the inherent damping in the system,

$\boldsymbol{f_{damper}}$ is the vector of forces in the structure due to the dampers, and

$\boldsymbol{f_{NL}}$ is the vector of nonlinear restoring forces in the structure.

$\boldsymbol{\ddot{u}(t), \dot{u}(t)}$ are the relative accelerations and velocities of the system.

Depending on how $\boldsymbol{f_{damper}}$ is represented in the analytical formulation, the viscously-damped system may be analytically classified as either a pure-viscous system or as a Maxwell system. As the focus of this paper is only design, the classical Maxwell model is used for the design problem formulation.

3.1 Viscous damper modelling

Figure 2 shows a nonlinear viscous damper modelled as a dashpot mechanism.

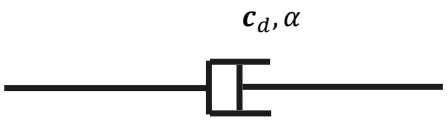

Figure 2: A viscous damper with "pure-viscous" modelling

When dampers are modelled as viscous, the EOM in Eq. 1 becomes:

$$\boldsymbol{M\ddot{u}(t) + C_{structure}\dot{u}(t) + C_d\dot{u}(t)^{\alpha} + f_{NL}(t) = -MI\ddot{u}_g(t)} \quad (2)$$

Note that, depending on the value of α, Equation 2 represents a system with potentially both structural and damping nonlinearity.

3.2 Maxwell damping

A more realistic modelling of a viscously-damped system uses a Maxwell model (Figure 3) in which the flexibility within the damper plus that of its supporting structure is represented explicitly.

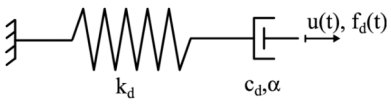

Figure 3: A Maxwell model of a viscous damper

The spring is in series with a dashpot which has a pure-viscous behaviour. This model is more difficult computationally as the spring and dashpot are in series so the force in the spring and dashpot are the same. The relative displacement and velocity across the model is the sum of the displacements and velocities of the dashpot and the spring, but the dashpot has no inherent stiffness and so the distribution of displacement in the spring and dashpot is not explicitly defined. This distribution has to be resolved by iteration or by some other solution approximation.

With the Maxwell model incorporated, Eq. 1 becomes:

$$\left.\begin{aligned} \boldsymbol{M\ddot{u}(t) + C_{structure}\dot{u}(t) + f_{damper}(t) + f_{NL}(t) = -MI\ddot{u}_g(t)} \\ \boldsymbol{\dot{f}_{damper}(t) = \Gamma(\dot{u}(t), k_d, c_d, \alpha)} \end{aligned}\right\} \quad (3)$$

In a normal time-history analysis the semi-discretized equations given in Equations 2 and 3 are temporally discretised and solved using implicit integration schemes.

4 A CRITICAL REVIEW OF THE CLASSICAL PSEUDO-STATIC DESIGN APPROACH

The traditional approach to the design of a structure incorporating viscous dampers estimates an effective modal damping ratio and arrives at the damper coefficients assuming a first-mode approach. The motivation for the development of this pseudo-static approach is that the majority of seismic engineering design relies on a single-mode approach. Also, the seismic forces in the majority of cases are represented using a response spectrum approach. The reduction in the response is then evaluated by superposing the effective modal viscous damping on the effective hysteretic damping of the structure.

Although it is a convenient way for designing the conventional systems without damping devices, for structural systems with additional mechanical damping devices this approach is an over-simplification. In most cases, this approach violates the physics of the problem at the outset because of the following:

1. When viscous dampers are introduced to the structure, the system becomes non-classical (i.e., classical modal dynamics are invalid as there is no single-basis real valued eigen/Ritz vector to diagonalise the system matrices). Simply, this means that there are neither normal frequencies nor mode shapes of free-vibration. The net effect is that no unique definition exists either for a single-degree-of-freedom system or for an effective damping ratio.
2. If classical modal dynamics is invalid, the classical response spectrum approach is also invalid and hence an approach of secant linearisation (in which the effective damping computation as a summation of hysteretic and viscous) becomes erroneous.
3. Dampers are sensitive to the phenomenon of inherent inelastic modal migration. As they introduce mechanical nonlinearity in parallel to the structural nonlinearity, they introduce phasing effects (i.e., the dampers can increase the response rather than reducing it - energy is retained in the structure rather than being dissipated). One of the aims of a damper design process is to minimize these phasing effects. A simplified single-mode-based approach completely misses this aspect.

5 MULTI-MODAL DYNAMICS AND PERFORMANCE-BASED DESIGN APPROACH FOR VISCOUS DAMPERS

As described in Section 4, an efficient design approach for viscous dampers requires a technique which can address the multi-modal dynamics directly.

One of the ways of doing this is to bind the performance objectives within an optimization framework and address the multi-modal dynamics directly. In such a process, a multi-objective, multi-modal design problem can be formulated as below:

$$\left.\begin{array}{c} Min\ \left(\Gamma_1(\boldsymbol{k_d},\boldsymbol{c_d},\alpha),\Gamma_2(\boldsymbol{k_d},\boldsymbol{c_d},\alpha),\ldots\ldots\Gamma_n(\boldsymbol{k_d},\boldsymbol{c_d},\alpha)\right) \\ subject\ to,(in\ continuum\ generic\ format) \\ \boldsymbol{\rho A\ddot{w}(x,y,z,t)+\frac{\partial^2}{\partial x^2}\left(\int_0^L\int_0^t C(x,\epsilon,t-\tau)\frac{\partial}{\partial\tau}\left(\frac{\partial w(\epsilon,\tau)}{\partial\epsilon}\right)d\tau d\epsilon\right)+f_d(k_d,c_d,\alpha,x,y,z,t)+E(\varepsilon,\gamma)I(x,y,z,t)w''''} \\ \boldsymbol{=f_g(x,y,z,t)} \\ \boldsymbol{\Xi_{constraint}\leq 1.0} \\ \boldsymbol{w(0)=\dot{w}(0)=0} \\ \boldsymbol{0\leq c_d} \end{array}\right\} \quad (4)$$

In this framework, Equation 4 above is semi-discretised and incrementally-solved temporally to obtain the design parameters of the dampers and the structure provided there is provision to add additional strength/stiffness.

In the design of the case study structure, Equation 4 was explicitly implemented.

6 CASE-STUDY STRUCTURE

6.1 Description of the structure

The 11-storey reinforced case-study structure is an amalgam of an existing eight-storey framed building and three storeys which will be added. The 3D Analytical model of the structure is comprised of beams and columns represented by shear-enhanced Euler beam elements. Shear walls are represented by fibre elements. The nonlinear behaviour of the super structure is modelled.

Dampers are only applied in the transverse (short) direction and are modelled as Maxwell viscous nonlinear elements with response nonlinearity. The Maxwell stiffness and damping is explicitly addressed in the design process.

No boundary nonlinearity or foundation effects were considered in the modelling. A fixed-boundary condition was used. The justification for this is that the foundations are on good soil (subsoil class B) and each foundation element is tied into all other foundation elements by ground beams.

Figure 4 below shows the line-element model of the structure.

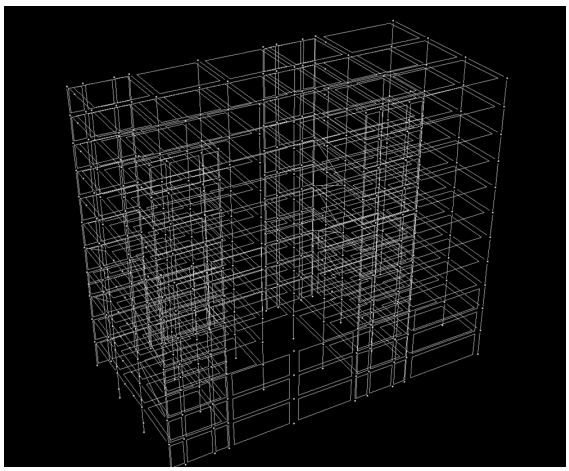

Figure 4: 3D frame-element model of the structure

6.2 Ground motions used for the study

A suite of seven earthquakes recommended (by Oyarzo-Vera, C et al., 2012) for Wellington were scaled in accordance with NZS1170.5. Of these, the Lucerne site records of the Landers (1992) earthquake exhibit the biggest velocity pulse associated with forward directivity - this being particularly appropriate for a Wellington CBD site where a near-fault factor applies. The Arcelik (1999) record was rejected as the NZS1170.5 scaling factors K1 and K2 were out of the acceptable range as per Clause 5.5.2. In addition, we included the records for El Centro 1979 and Yarimka (1999) as they have forward-directivity characteristics. The main purpose for their inclusion was to test the robustness of the viscous damper design. S_p=1.0 is used for the present study.

6.3 Highly efficient "sizing" and distribution of viscous dampers

Viscous dampers were efficiently sized and distributed up the height of the structure using the design approach described in Section 5. This process results in a highly efficient distribution of 12 viscous dampers distributed in two bays (six in each bay) up the height of the structure and satisfying a set of *performance objectives* explicitly. The smaller number of dampers results in reduced interference with the architecture and does not affect the functionality. Also, as the design uses a sophisticated framework described in Section 5 which follows closely the dynamics of the system, a highly-sustainable design is obtained in terms of material consumption (initial investment) and efficiency in reducing damage (seismic loss).

6.4 Results and discussions

6.4.1 Global responses: Inter-storey drift response

Inter-storey drifts were computed for the suite of all eight earthquakes of which three are near-fault types. Earthquakes were applied as bi-directional ground motions and their directions were swapped to cover the worst response. Figure 5 shows the inter-storey drift ratio plots for the earthquakes scaled to design-basis earthquake (DBE) and maximum considered earthquake (MCE) levels. The DBE for this structure is 130 % ULS for Importance Level 2. A total of 32 analyses were performed to generate the curves in Figure 5. As the structure is viscously damped, an inherent modal damping of 3 % was assumed in the system for the DBE calculations. For the MCE evaluation, more deformation is expected to occur and so a higher damping ratio of 5 % was assumed. This is justified as per Chopra (2014). It must be noted that, in the case of the MCE excitations, where a factor of 1.8 is applied to the DBE excitation level, more damping will be exhibited by the combined soil-structure system. As dampers only change the amplitude of the global undamped modes, even with soil compliance, the system is expected to work. This is very much in contrast to a base-isolated structure where soil compliance could mean a phenomenon called soil-foundation-isolator-structure (SFIS) interaction might occur and which is more difficult to quantify. The main reason for this is that base-isolation nonlinearity modifies the boundary condition of the system thereby making use of classical modes of free-vibration invalid - whereas viscous dampers do not modify either the mass or stiffness and hence no effect on the natural mode shape.

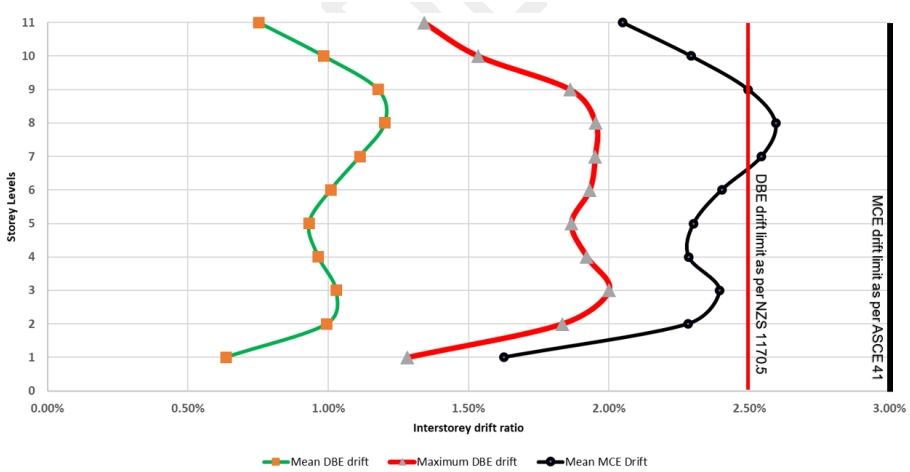

Figure 5: Inter-storey drift ratio for DBE and MCE levels

In Figure 5, the mean DBE drift ratio is the average of the drift ratio for each storey across all eight earthquakes; the maximum DBE drift ratio is the maximum/envelope of the drift ratios for each storey across all earthquakes; the mean MCE drift ratio is the average of the drift ratio for each storey across all earthquakes. As can be seen, all DBE drift ratios were found to be below the NZ 1170.5 limit of 2.5 %, and the mean MCE drifts were below the 3 % allowed by ASCE 41. As the plastic hinge strains are still below 2 %, the analysis, even in an MCE, is a large-displacement-small-strain one represented by the string stiffness $P-\Delta$ formulation (i.e., a pseudo geometric stiffness). It is important to note that the peak drift ratio was recorded in the Lucerne earthquake which has a forward-directivity pulse. More discussion is presented in Section 6.4.3 on this aspect of drift.

6.4.2 Global response: Incremental Dynamic Analysis (IDA)

Adding viscous dampers to the structure makes the system damping nonclassical as explained in Section 4. Proportional equivalent-damping spectral reductions are not reflective of the effect of the dampers on the structure as the equivalent viscous-damping-ratio-based spectral reductions do not reflect the *phasing effects*. However, an acceleration-displacement response spectrum (ADRS) type of assessment gives a qualitative picture of the efficiency of the viscous dampers – provided that the system backbone is generated using non-linear dynamic analysis. This section describes how an IDA-based backbone was generated and plotted in the ADRS domain to give a qualitative picture of the performance of the damped structure.

The dynamic backbone was generated for lateral loading of the structure in the transverse direction by performing inelastic dynamic analyses in which the scaling of the input ground motion was incrementally and monotonically increased. The same suite of eight ground motions was used. This backbone is the dynamic counterpart of a static pushover backbone. Although an effective single-degree-of-freedom (SDOF) system has thus been created, its generation incorporates inelastic dynamic analyses. The structure has been subjected to up to two times the 130 % DBE level (i.e. 260 % DBE). The structure does not exhibit any collapse tendencies. A total of 64 analyses were performed to generate the backbone. The P-delta effect was considered. As the intensity increases, the plastic-hinge strains increase, and the qualitative nature of the results increases - especially for large-intensity earthquakes.

Figure 6 shows the Acceleration-Displacement Response Spectrum (ADRS) plot.

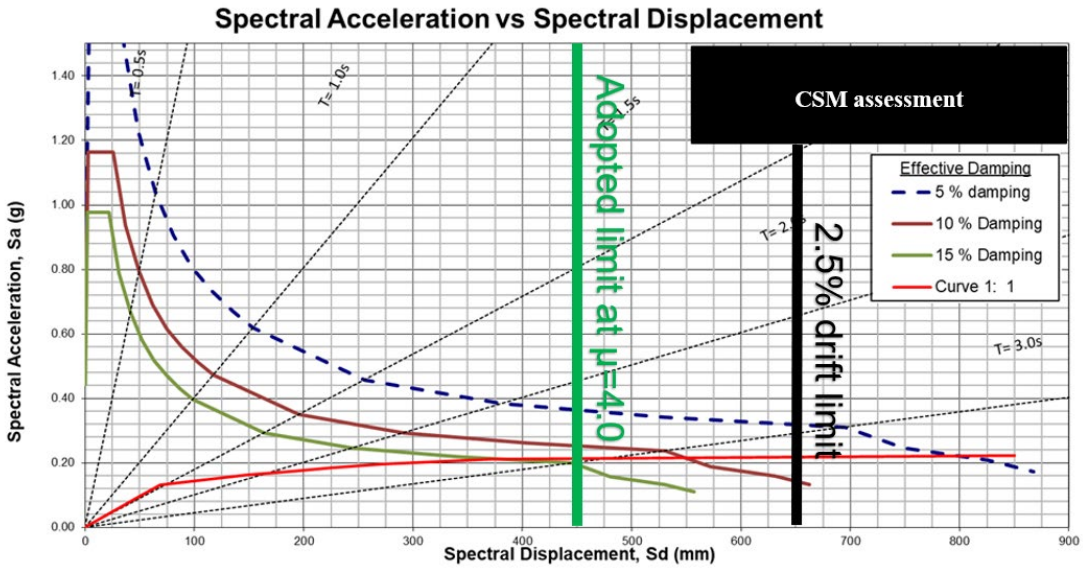

Figure 6: Dynamic Capacity Spectrum Assessment

The ADRS plot was generated for the effective, inelastic, SDOF system with an approximate modal height calculated as per Priestley et al. (2007) at 0.67 times the total height of the structure. The peak base shear was recorded for the peak inelastic modal displacement of the structure. The black line in the plot indicates the 2.5 % modal drift point. An average displacement ductility of six was exhibited by the structure. Considering a confidence factor (EC8 part 3) of 1.5, only a system ductility of 4 was assumed for the calculation of hysteretic damping. Considering the structure to be a reinforced-concrete structure with plastic hinges modelled by Takeda hysteresis loops, damping was estimated, as per Grant et al. (2005), to be 15 %. The vertical green line represents the performance point. It is notable that the structural backbone exhibits a high displacement capacity (up to a factor of 2) after the green line. This indicates that the damped structure may exhibit good seismic resilience in general. In the generation of the backbone we also considered the effect of structural inertia; in a conventional pushover, no inertia effects are considered.

6.4.3 Local responses: near-fault event vs. far-field event: some observations

Figure 7a shows a typical beam-hinge response exhibited by the structure in the Lucerne earthquake (near-fault earthquake). Figure 7b shows the same hinge response for a far-field event. As can be seen, more cyclic behaviour is being exhibited by the hinges in this type of event when compared to the near-fault response.

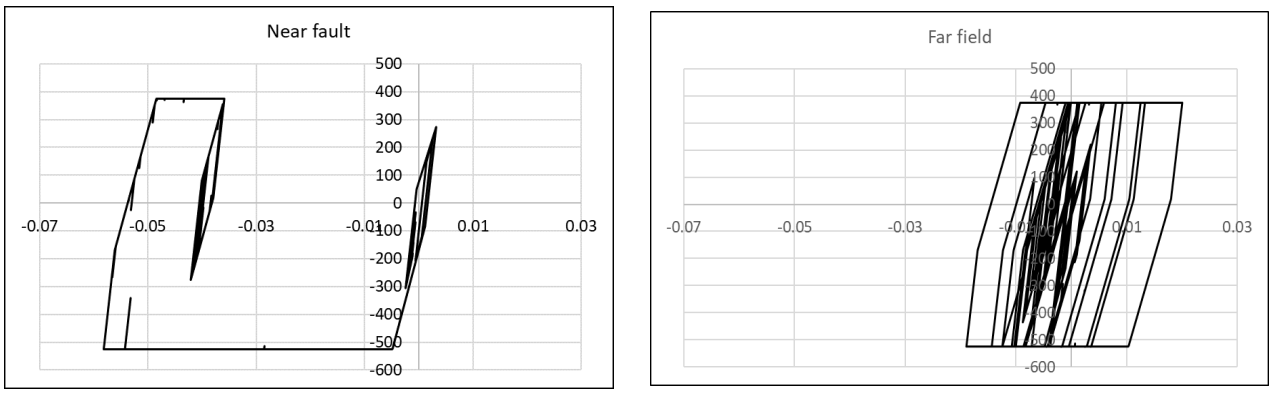

a) b)

Figure 7: Plastic hinge hysteresis a) near-field earthquake b) far-field earthquake

The far-field loop shows a large amount of energy dissipated by the closed hysteresis loops whereas the hysteresis shown for the Lucerne earthquakes exhibits very few closed loops with very small, enclosed area - implying very little energy dissipated by the members.

6.5 Some critical observations based on the results

The results have shown the significance of considering the time-history analyses directly. Some key points are discussed below.

6.5.1 Peak inter-storey drift vs. average inter-storey drift

ASCE 41 allows the seismic performance to be estimated as either the maximum of drifts due to three earthquakes or the mean value of demands due to a minimum of 11 earthquakes. This requirement is a little ambiguous because engineers in practice tend to average out the near-fault event drifts by including those from the far-field events. For locations such as Wellington with near active faults, this can have a huge effect as there is a high likelihood of experiencing motions similar to Landers 1993 which has a ground displacement of 2.5 m or more at a velocity of approximately five times that of a normal far-field earthquake. It is the opinion of the authors that, if the average is to be used, only earthquakes of a similar type should make up the suite of 11 ground motions *and then there should be two groups - one with and one without forward-directivity effects.* Alternatively, the peak responses using fewer earthquake records could be considered.

In this study, we have considered the peak of all eight earthquakes to be below a certain threshold.

One other aspect is that Clause 7.3.1.2 in NZS 1170.5 allows a factor of 0.67 to be applied in the case of inter-storey drift when a near-fault event is considered. Although no specific explanation can be found in the standard's Commentary, the intention may have been to reflect the fact that a near-fault event has a huge velocity spectrum which, in the course of the earthquake, actually migrates it from a DBE to something like an MCE; however, as the factor is only applied on the response side (only to the drift), it does not directly translate to the hinge rotations and other aspects of the analysis and completely misses the performance objective. It is the opinion of the authors that the application of the factor might need to be investigated further and a more prudent approach might be to apply it on the demand side rather than on the capacity side by amalgamating it with the existing structural performance factor, S_p.

6.5.2 Near-fault hinge response vs. far-field hinge response

As shown in Figure 7a, the plastic hinges that appear during a near-fault event do not have a closed loop behaviour whereas the hinges in Figure 7b exhibit more cyclic behaviour. This means that the effective damping ratio may be considerably less than anticipated for a near-fault event in the current design process for both force-based and displacement-based methods. This observation is also important for conventional design of undamped structures - mainly because, in a conventional single-mode approach (i.e., code-type) design philosophy, an effective damping ratio is calculated assuming that full cycles are being generated during a ground motion. This aspect of the near-fault characteristic is recognised partially in displacement-based design of conventional structures (Priestley 2007). The multi-inelastic modal effect happening due to this phenomenon is difficult to address in the present conventional design framework. This aspect needs to be investigated thoroughly before incorporating it in future codes. It becomes more important for a viscously-damped structure subjected to a near-fault event mainly because the dampers work on the inter-storey drift velocity. This means that the design of a viscously-damped structure must include consideration of inelastic dynamic effects.

6.5.3 Incremental equilibrium analyses versus total equilibrium analyses

A review of the PERFORM-3D analyses was undertaken by an independent team using parallel, fully-fledged, 3D analyses performed with Ruaumoko3D (Carr 2017). All the early Ruaumoko analyses failed with the loss of equilibrium, especially for the Landers near-fault earthquake in which the structure had a high degree of mechanical and structural nonlinearity. On detail investigation, it was found that some columns had tensile forces imposed on them far exceeding the axial capacity of the columns. With the consequent reduction in the column moment capacity, the shear forces shed by those columns could not be carried by adjoining columns and the structure was not able to maintain full equilibrium within the Ruaumoko total equilibrium solution strategy. If yield in the foundation beams is allowed at the bases of the interior columns in the analysis model, the column axial loads are limited – thus allowing some column moments to develop. This, combined with *a judicious optimal sizing and placement of the dampers in the frames*, resulted in a more stable de-sensitized system.

The main reason for this discrepancy was that the incremental equilibrium dynamic analysis framework adopted by PERFORM-3D does not consider this total equilibrium problem. In incremental equilibrium, no complete/total system equilibrium is checked at every time-step; in other words, the equilibrium is only satisfied within the time-step increment. No total equilibrium check is done as no damping actions are computed.

Most commercial dynamic time-history analysis software platforms follow the classical Newmark incremental equilibrium (Clough *et al.*, 1993) and these run the risk of drifting away from a state of equilibrium during the analysis process. The solution strategy in Ruaumoko was changed in 1984 to one where the incremental displacement is such that dynamic total system equilibrium is achieved at the end of the time-step. The resulting system is one that is always ensuring dynamic equilibrium of the structure at every time-step. This is not possible in most dynamic time-history commercial software as these programs do not compute the structural damping actions during the analyses and therefore cannot ensure total system equilibrium. In Ruaumoko, after finding the difficulties with the traditional Rayleigh damping model in 1978, the damping actions have always been available and thus the change in approach was relatively straightforward. These analyses of the building in Wellington have been a further step in a learning curve emphasising the difficulties in the traditional incremental equilibrium approaches.

This discrepancy between the two sets of analyses was very similar to problems encountered in 1984 whilst modelling a stack of containers rocking on a concrete floor in an earthquake in an incremental Newmark solution strategy. The corners of the containers, after impacting the concrete floor, were given large vertical velocities that resulted in large vertical velocities and, as vertical equilibrium was not checked, they never came back. The solution strategy was changed from satisfying incremental equilibrium within the time-step to achieve total dynamic equilibrium at the end of the time-step.

7 CONCLUSIONS

The design process for including viscous dampers as part of the retrofit and extension of a reinforced concrete structure in Wellington emphasized the need for careful attention to both the potential for near-fault earthquakes to have a significant impact on structures with and without dampers and to the importance of avoiding phasing effects in viscously-damped structures.

The optimising process followed resulted in not only a very efficient design with respect to the relatively small number of dampers required, but also gave the designers confidence that the final design is more reliable in outlier earthquakes than would be achieved by a simple first-mode, response spectrum approach using an estimate of percentage damping enhancement.

The independent peer review of the nonlinear time-history analyses used to confirm the code compliance of the damped structure highlighted that some commonly-used computer programs do not have checks on total equilibrium at each time-step. Such programs may not be able to model viscously-damped structures during the periods when the structure is also experiencing significant inelasticity. At worst, the analyses may become unstable.

Recommendations have been made as to the desirability of changing NZS 1170.5 with respect to how near-fault earthquakes are treated in suites of appropriate records used to demonstrate code compliance.

A proper optimal design of viscous dampers that considers the inelastic dynamics of the system closely will result in a very sustainable solution with minimum material and architectural interference.

References

Carr, A.J, 2017. *Ruaumoko3D Users Manual*. Carr Research Ltd. 215 p.

Chopra A.K. 2014. *Dynamics of Structures: Theory and application to Earthquake Engineering*, Prentice Hall.

Clough, R.W. & Penzien, J., 1993. *Dynamics of Structures*, 2nd Edition, McGraw-Hill, 1993.

Constantinou, M.C., Syman, M.D., Tsopelas, P., Taylor D.P., 1993. *Fluid viscous dampers in applications of seismic energy dissipation and seismic isolation*. ATC-17-1.581-591.

Grant, D.N., Blandon C.A., Priestley, M.J.N, 2005. *Modelling inelastic response in direct displacement design*, Report 2005/03, IUSS Press, Pavia,104 pp.

NZS1170.5:2004 (2004). Structural Design Actions - Part 5: Earthquake design actions. New Zealand, Standards New Zealand.

Oyarzo C., McVerry,G.,& Ingham J., 2012. *Seismic zonation and default suite of ground-motion records for time-history analysis in the North Island of New Zealand*. Earthquake Spectra, 28(2), 667–688.

Pampanin, S., 2015. *Towards the "ultimate earthquake-proof" building: development of an integrated low-damage system.* 321-358. http://dx.doi.org/10.1007/978-3-319-16964-4_13.

Powell G., 2006, PERFORM 3D, User Guide,

Priestley, M.J.N., 2007. *Displacement-based seismic design of structures*. IUSS Press.

Wada, A., Huang,Y., & Bertero, V.V., 2004. *Innovative Strategies in Earthquake Engineering*. Bozorgnia.

Y., Bertero, V.V.,(Ed), *Earthquake Engineering, From Engineering Seismology to Performance-Based Engineering*, (pp. 10-1-10-33). CRC Press, London.